Electronic Supplementary Information (ESI) for

Facile synthesis of highly active and durable PdM/C (M = Fe, Mn) nanocatalysts for oxygen reduction reaction in alkaline medium

Yaovi Holade,[a] Rodrigo G. da Silva,[a,b] Karine Servat,[a] Teko W. Napporn,[a] Christine Canaff,[a] Adalgisa R. de Andrade,[b] and Kouakou B. Kokoh*[a]

*Corresponding author: boniface.kokoh@univ-poitiers.fr

A°) Description of the method used for the evaluation of ECSA

The electrochemical active surface area (ECSA) is used to compare different catalyst and to normalize the kinetic current. In literature, various methods can be used to determine ECSA of metals: adsorption/desorption of hydrogen (if it exists), stripping of probe molecule (CO, if it is possible), stripping of under potential deposition (UPD) or reduction of oxide.[1] It is well-known that Pd (and in particular PdNPs) has the ability of absorbing hydrogen into its crystal lattice.[2] For avoiding this phenomenon, we did not use the hydrogen adsorption/desorption region method but the reduction peak of palladium oxide (PdO) to determine ECSA. A charge density of 424 µC cm^{-2} (Q_m) was associated to the reduction of the formed PdO monolayer.[3] Figure S1 shows the integrated region of interest. The exchange charge (Q_{ex}) from Eq. (1) can be assessed by two independent methods either using "integration approach" (*e.g.* Origin® software) or the old method namely "weighing method or Lavoisier's approach" from Eq. (2).[4] The "weighing method" uses a tracing paper as reference for weighing on an ultra-sensitive balance. Briefly, it involves cutting a known surface of tracing paper (s_0) and weighing it. The variables ***a***, ***b***, ***x***, ***y*** and ***v*** used in Eq. (2) are represented in Figure S1. The variable m_0 is the weight of this tracing paper while m_1 is the weight of the shaded curve printed on any paper and modeled (on the tracing paper). Eq. (3) corresponds to the calculation of the active surface area in **cm^2**.

$$Q_{ex} = \frac{1}{v}\left(\int_{E_{onset}}^{E_{end}} i(E)dE\right) \quad (1)$$

$$Q_{ex} = \frac{m_1}{m_0} \times \frac{s_0}{x \times y} \times \frac{a \times b}{v} \quad (2)$$

$$SA(cm^2) = \frac{Q_{ex}}{Q_m} \quad (3)$$

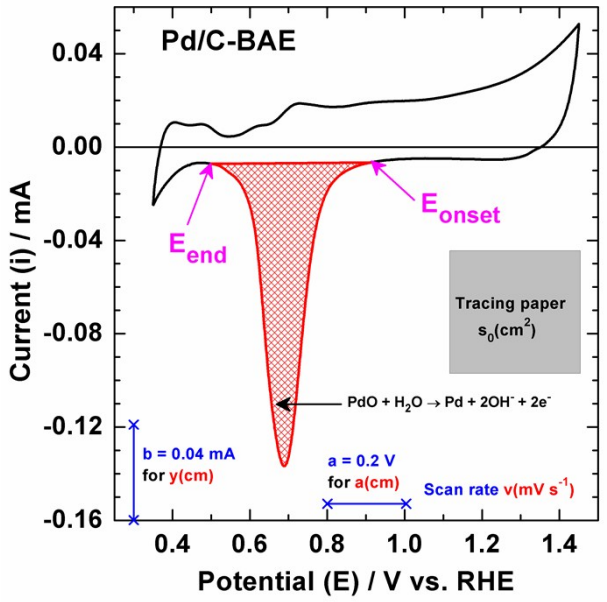

Fig. S1 Illustration of the method used for ECSA evaluation by CV: 5 mV s^{-1}; 0.1 mol L^{-1} KOH.

B. Fundamentals of Oxygen Reduction Reaction in aqueous medium

B-1. General concepts

The different steps of ORR in aqueous medium (pH = 0-14) can be found in many reviews.[5] The overall reaction for the direct four-electron pathway, which takes place in alkaline medium is described by Eq. (1) and involves the redox couple O_2/HO^-.

$$O_2 + 2H_2O + 4e^- \rightleftharpoons 4HO^- \quad (4)$$

The theoretical point in experimental conditions where the ORR, as any electron-driven reaction should start is called the *equilibrium potential* (E_{eq}) that is defined as the *potential at zero current*. E_{eq} is a thermodynamic parameter and can be numerically calculated from the Nernst equation,[6] by Eq. (5) in alkaline medium. Remember that in this case, the potential is scaled with the Standard Hydrogen Electrode (SHE).

$$E_{O_2/HO^-}/(\text{V vs. SHE}) = E^0_{O_2/HO^-} + \frac{RT}{4F}\ln\left\{\frac{C_{O_2}}{C^0}\left(\frac{C^0}{[HO^-]}\right)^4\right\} \quad (5)$$

C^0(= mol L^{-1}): reference molar concentration. R(= 8.314 J K^{-1} mol^{-1}): gas constant. T(= 273.15+ θ, where θ is the temperature in °C): temperature in Kelvin. F(= 96 485 C mol^{-1}): Faraday's constant. C_{O_2} (mol L^{-1}): oxygen solubility. $E^0_{O_2/HO^-}$ (= 0.399 V vs. SHE) is the standard equilibrium potential of O_2/HO^-.

Note that SHE is a virtual reference electrode and cannot be fabricated experimentally because it involves standard conditions (1 bar, pH = 0).[7] So, during ORR experiments, many reference electrodes are currently used. Depending on the electrolytic medium (which induces the pH value, and chemical species constant change), it is more convenient to convert these values *versus* the Reversible Hydrogen Electrode (RHE). In the case of SHE, the conversion of the equilibrium potential into RHE is described by Eq. (6) in alkaline medium.

$$E_{eq} = E_{O_2/HO^-}/(\text{V vs. RHE}) = \left(E^0_{O_2/HO^-} + \frac{RT}{4F}\ln\left\{\frac{C_{O_2}}{C^0}\left(\frac{C^0}{[HO^-]}\right)^4\right\}\right) - \left(E^0_{H^+/H_2} + \frac{RT}{4F}\ln\left\{\left(\frac{[H_3O^+]}{C^0}\right)^4\right\}\right)$$

$$E_{eq} = E_{O_2/HO^-}/(\text{V vs. RHE}) = E^0_{O_2/HO^-} + \frac{RT}{4F}\ln\left(\frac{C_{O_2}}{C^0}\times\frac{1}{Ke^4}\right) \quad (6)$$

where $E^0_{O_2/HO^-} = 0.399\ \text{V vs. SHE}$, $E^0_{H^+/H_2} = 0.000\ \text{V vs. SHE}$ and Ke = 10^{-14} (in SI unit) at 25 °C.

All the important data involved in the ORR results are gathered in **Table 1**. It is obvious that any change of the experimental conditions induces a variation of E_{eq}.

Table S1. Fundamental basic data of the ORR at 25-50 °C in different supporting electrolytes.

Electrolyte solution (25 °C, 1 atm)	**E_{eq}[a] (V vs. RHE)**	**D_{O2}[b] ($cm^2\ s^{-1}$)**	**υ[b] ($cm^2\ s^{-1}$)**	**C_{O2}[b] ($mol\ cm^{-3}$)**
0.5 M H_2SO_4 (Refs.[8])	1.184	2.01×10^{-5}	1.07×10^{-2}	1.03×10^{-6}
0.1 M $HClO_4$ (Refs.[8a,8c,9])	1.185	1.93×10^{-5}	1.01×10^{-2}	1.26×10^{-6}
0.1 M NaOH (Refs.[8c,8d])	1.183	1.90×10^{-5}	9.97×10^{-3}	8.35×10^{-7}
0.1 M KOH (Refs.[8c,8d])	1.185	1.90×10^{-5}	1.00×10^{-2}	1.2×10^{-6}
[a] Calculated from Nernst-based equations. [b] From the indicated literature references.				

B.2. Data analysis through ORR equations

Assuming a planar electrode or a thin film (RDE/RRDE), the use of Koutecky-Levich equation (KL) implicitly requires the two criteria: (i) The existence of an electron transfer process that is the rate determining step *rds*; (ii) the reaction is of a first-order reaction with respect to the electro-reactive species (O_2). The above specific conditions are met in the mixed control regime. Thus, the kinetic current density (j_k) and the current density related to mass transport process (j_l^{diff}) give the total current density (j) as the sum of reciprocals, Eq. (7). This expression is known as the Koutecky-Levich equation.[8b,8d,10] It should be noticed that all the current densities are normalized with the geometric surface area.

$$\frac{1}{j} = \frac{1}{j_l^{diff}} + \frac{1}{j_k} = \frac{1}{j_l^{diff}} + \frac{1}{j_l^{film}} + \frac{1}{j_l^{ads}} + \frac{1}{j_0 \frac{\theta}{\theta_{eq}} e^{\frac{\eta}{b'}}} \tag{7}$$

$$j_k^{app} = j_0 \frac{\theta}{\theta_{eq}} e^{\frac{\eta}{b'}};\ \eta = E - E_{eq};\ b' = \frac{RT}{\alpha n F};\ j_l^{diff} = n_{ex} B \Omega^{\frac{1}{2}} \quad \text{where} \quad B = 0.201 F \upsilon^{-\frac{1}{6}} C_{O_2} D^{\frac{2}{3}}$$

- j: measured ORR current density at the disk ($mA\ cm^{-2}$),
- j_l^{diff} : diffusion-limiting current density of O_2 in the bulk electrolyte ($mA\ cm^{-2}$),
- j_l^{film} : diffusion-limiting current density of O_2 inside the film of the catalytic ink ($mA\ cm^{-2}$),
- j_l^{ads} : diffusion-limiting current density associated with O_2 adsorption at the active site ($mA\ cm^{-2}$),
- j_k : kinetic current density, that is free from the mass transport ($mA\ cm^{-2}$)
- j_0 : exchange current density ($mA\ cm^{-2}$),
- n_{ex}: overall exchanged electrons number (total),
- n: number of transferred electrons during the *rds* ($n \le n_{ex}$),
- b': Tafel slope (V),
- α: symmetric factor or the charge transfer coefficient ($0 < \alpha \le 1$)

- $\eta = |E - E_{eq}|$, overpotential (V),
- θ, θ_{eq}: degree of coverage of the catalyst surface (active sites) by oxygen at potential E and at the equilibrium potential E_{eq}, respectively,
- D_{O_2} : diffusion coefficient of O_2 in solution ($cm^2\ s^{-1}$),
- C_{O_2} : the bulk concentration of O_2 in the electrolyte (10^{-3} mol cm^{-3}),
- υ: kinematic viscosity of the electrolyte ($cm^2\ s^{-1}$),
- F: Faraday's constant (F = 96485 C mol^{-1}),
- Ω: RRDE speed (rpm).

The electrochemical and hydrodynamic properties of RDE/RRDE are correlated with the KL equation that can be expressed by Eq. (10). It becomes thereafter Eq. (9) when $\Omega \rightarrow \infty$. This relation enables getting experimentally the kinetic current density (j_k).

$$\frac{1}{j} = \frac{1}{n_{ex} B \Omega^{\frac{1}{2}}} + \frac{1}{j_l^{film}} + \frac{1}{j_l^{ads}} + \frac{1}{j_k^{app}} \quad \Rightarrow \quad \lim_{\Omega \to \infty} \left(\frac{1}{j}\right) = \frac{1}{j_l^{film}} + \frac{1}{j_l^{ads}} + \frac{1}{j_k^{app}} \tag{8}$$

$$\frac{1}{j_k} = \frac{1}{j_l^{film}} + \frac{1}{j_l^{ads}} + \frac{1}{j_k^{app}} \tag{9}$$

$$\frac{1}{j} = \frac{1}{n_{ex} B \Omega^{\frac{1}{2}}} + \frac{1}{j_l^{film}} + \frac{1}{j_l^{ads}} + \frac{1}{j_k^{app}} \quad \Rightarrow \quad j^{-1} = (n_{ex} B)^{-1} \Omega^{-\frac{1}{2}} + j_k^{-1} \tag{10}$$

From Eq. (10), the curve j^{-1} *versus* $\Omega^{-\frac{1}{2}}$ that is known as "Koutecky–Levich plot" is a straight line characterized by a KL slope $\alpha_{KL} = (n_{ex} B)^{-1}$ and a KL intercept $\beta_{KL} = j_k^{-1}$. The slope of the straight line enables extracting the total number of exchanged electrons ***n*****ex*** and the intercept at the origin ($\Omega \rightarrow \infty$) gives the inverse of the kinetic current $\mathbf{j_k}$. The determined $\mathbf{j_k}$ from the intercepts is expressed in *mA per cm²* of disc (sample), referred as "absolute activity".[11] Then, and as recommended,[11] j_k must be normalized as:

(i) the "area-specific activity" ***A*****s*** (mA per cm² metal: $\mathrm{mA\,cm^{-2}_{metal}}$ or $\mathrm{mA\,cm^{-2}_{real}}$) by dividing the absolute activity by the surface-area enhancement factor,

(ii) the "mass activity" ***A*****m*** (mA per µg of metal: $\mathrm{mA\,\mu g^{-1}_{metal}}$) by dividing the absolute activity by the metal loading.

The surface-area enhancement factor (also referred as the electrochemical surface roughness or electrode roughness) is the ECSA of the catalyst divided by the planar area of the sample (cm^2 metal per planar cm^2).

In the KL equation, especially in Eq. (9), it is impossible to separate contributions from j_l^{film} and j_l^{ads} since they do not depend on the rotation rate. They are gathered as j_L (Eq. (11)) that is

defined as a *limiting current density resulting from a mixed-control by the diffusion of O_2 inside the film of the catalytic ink and by the adsorption of O_2 at the active sites*. The expression of j_k becomes thereafter Eq. (13), a relationship between j_L and j_k^{app}.

$$\frac{1}{j_L} = \frac{1}{j_l^{film}} + \frac{1}{j_l^{ads}} \tag{11}$$

$$\frac{1}{j_k} = \frac{1}{j_L} + \frac{1}{j_0 \frac{\theta}{\theta_{eq}} e^{\frac{\eta}{b'}}} \tag{12}$$

$$\frac{1}{j_k} = \frac{1}{j_L} + \frac{1}{j_0 \frac{\theta}{\theta_{eq}} e^{\frac{\eta}{b'}}} = \frac{1}{j_L} + \frac{1}{j_0 \frac{\theta}{\theta_{eq}} e^{-\frac{E-E_{eq}}{b'}}} \quad \Rightarrow \quad \lim_{\eta \to \infty}\left(\frac{1}{j_k}\right) = \frac{1}{j_L} \tag{13}$$

Eq. (12) becomes thereafter Eq. (13) when $\eta \to \infty$, meaning $E \ll E_{eq}$ because $E < E_{eq}$ for reduction reactions like ORR. Therefore, j_L is determined experimentally after extrapolating the reported j_k^{-1} values as a function of the potential E.

Supposing that the coverage of the catalyst surface (active sites) by O_2 at potential E and at the equilibrium potential E_{eq} is quite the same ($\theta \approx \theta_{eq}$), Eq. (12) becomes relationship Eq. (14). If there is no competitive reaction involving the catalyst surface in the whole potentials range of interest, the experiments will meet the hypothesis by bubbling continuously O_2.

$$\frac{1}{j_k} = \frac{1}{j_L} + \frac{1}{j_0 e^{\frac{\eta}{b'}}} = \frac{1}{j_L} + \frac{1}{j_0 e^{-\frac{E-E_{eq}}{b'}}} \tag{14}$$

$$-\left(E - E_{eq}\right) = b' \ln\left(\frac{j_L}{j_0} \times \frac{j_k}{j_L - j_k}\right) \Rightarrow E - E_{eq} = \left[-b \log\left(\frac{j_L}{j_0}\right)\right] - \left[b \log\left(\frac{j_k}{j_L - j_k}\right)\right] \tag{15}$$

$$\alpha_{Tefel} = \frac{\partial \eta}{\partial\left(\log\left(\frac{j_k}{j_L - j_k}\right)\right)} \quad \Rightarrow \quad b = -\alpha_{Tefel} = b' \times \ln(10) \approx 2.3 \frac{RT}{\alpha n F} \tag{16}$$

$$\beta_{Tafel} = -b \log\left(\frac{j_L}{j_0}\right) \quad \Rightarrow \quad j_0 = j_L \times 10^{-\frac{\beta_{Tafel}}{b}} \tag{17}$$

Plotting either η or $(E-E_{eq})$ *versus* $\log\left(\frac{j_k}{j_L - j_k}\right)$ is known as "Tafel plot" (Eq. (15)) and is a straight line characterized by $\alpha_{Tafel} = \frac{\partial\left(E - E_{eq}\right)}{\partial\left(\log\left(\frac{j_k}{j_L - j_k}\right)\right)} = -b$ that enables getting the Tafel slope (expressed

in mV dec^{-1}) *via* Eq. (16) and the intercept $\beta_{\text{Tafel}} = -b\log\left(\frac{j_0}{j_L}\right)$ from which the exchange current density j_0 is determined through Eq. (17).

The major benefit of RRDE equipment for ORR is the determination of the reaction intermediate. A RRDE apparatus enables determining the reaction product formation efficiency at the disk that is typically H_2O (acid medium) or HO^- (alkaline medium), in direct relationship with the amount of the reaction intermediate (H_2O_2 or HO_2^-). The method was firstly developed by Jakobs et *al*.[12] in 1985 and then revised by Vork and Barendrecht in 1990.[13] During the ORR, O_2 is reduced at the disk (current: $I_D < 0$) and the intermediate H_2O_2 or HO_2^- is radially swept outward away from the disk and toward the ring where it is oxidized (current: $I_R > 0$). The set relationship is given by Eq. (18).[13] It is highly important to note that even if N is provided in percentage, *e.g*. 20.5% herein, it is used in fraction meaning N = 0.205. The O_2 reduction to H_2O involves 4e$^-$ and only 2e$^-$ when the reaction process leads to H_2O_2 (or HO_2^-). Thus, when both H_2O and H_2O_2 (or HO_2^-) are produced, n_{ex} is easily accessed through Eq. (19).[12,13]

$$p(H_2O) = 1 - p(H_2O_2) = \frac{NI_D + I_R}{NI_D - I_R} = \frac{1 - \frac{I_R}{N|I_D|}}{1 + \frac{I_R}{N|I_D|}} \tag{18}$$

$$n_{ex} = n_{(O_2 \to H_2O)} + n_{(O_2 \to H_2O_2)} = 4p(H_2O) + 2p(H_2O_2) = 2\left[p(H_2O) + 1\right] = \frac{4N|I_D|}{N|I_D| + I_R} = \frac{4}{1 + \frac{I_R}{N|I_D|}} \leq 4 \tag{19}$$

The complete ORR study requires a RRDE that has the advantage of analyzing the short-life intermediate in a steady-state measurement.[10b] To this end, one needs a *four-electrode potentiostat*, also referred as a *double/bi-potentiostat* that enables controlling the potential of the disc and the ring with respect to the reference electrode independently and measuring the current through each of them separately. Typically, the potential of the ring is hold at a fixed value (E_R) and that of the disk is varied to analyze the products formed at it surface by studying the ring current (I_R) as a function of the disk potential (E_D), or *vice versa*. RRDE must be calibrated by determining its *collection efficiency* ***N***, which is defined as the *fraction of a species formed at the disc that arrives at the ring and reacts there* [10b] It is specific to the RRDE geometry and does not depend on the studied redox reaction. The easy and elegant way to evaluate experimentally ***N*** consists of considering a simple reduction reaction, for example, Fe^{3+} to Fe^{2+} from $[Fe(III)(CN)_6]^{3-} + e^- \rightarrow [Fe(II)(CN)_6]^{4-}$. It is calculated from Eq. (20) only valid for currents, not the current densities! E_R must be higher than the potential where the involved intermediate is oxidized (*e.g*. 0.77 V vs. RHE for Fe^{3+}/Fe^{2+} system). For the ORR, E_R ~1.1-1.3 V vs. RHE.

$$N = -\frac{I_R}{I_D} = \frac{I_R}{|I_D|} \leq 1 \tag{20}$$

C. Additional Tables and Figures

Table S2. Comparative performances from ORR-RRDE experiments (0.1 M KOH) on the as-synthesized PdM/C (M = Fe, Mn) nanocatalysts during APCT. $E_{1/2}$ was graphically determined at 1600 rpm (E at i = I_D/2). Note: "BAE" refers to Bromide Anion Exchange and "Pol" refers to Polyol.

Electrode material at *p* cycle (k = 1000)		**$E_{eq(exp)}$**	**$E_{1/2}$ at** 1600 rpm	**Tafel slope b(mV dec^{-1})**		**j_0 (×10^{-3} mA cm^{-2})**		**at 0.85 V vs. RHE**		
								j_k		**n_{ex}**
p	**Catalyst**	V vs. RHE		Low η	High η	Low η	High η	mA cm^{-2}_{Pd}	mA mg^{-1}_{Pd}	
20	**Pd/C-BAE**	1.052	0.86	65	125	0.07	278	0.19	49	4.0
	PdFe/C-BAE	1.023	0.85	85	174	0.78	298	0.30	81	4.0
	PdFe/C-Pol	1.002	0.81	68	174	0.02	378	0.08	27	3.9
	PdMn/C-BAE	1.054	0.87	83	165	0.85	267	0.35	93	4.0
	PdMn/C-Pol	1.056	0.86	82	159	0.64	175	0.41	70	4.0
5k	**Pd/C-BAE**	1.057	0.85	70	125	0.06	78	0.16	39	4.0
	PdFe/C-BAE	1.022	0.84	83	157	0.62	140	0.18	56	4.0
	PdFe/C-Pol	0.993	0.80	69	168	0.02	237	0.07	24	3.7
	PdMn/C-BAE	1.047	0.86	81	161	0.55	222	0.29	71	4.0
	PdMn/C-Pol	1.053	0.85	79	158	0.34	154	0.29	60	4.0
10k	**Pd/C-BAE**	1.046	0.83	66	132	0.03	74	0.16	30	3.9
	PdFe/C-BAE	1.021	0.83	83	159	0.45	133	0.16	46	3.9
	PdFe/C-Pol	1.005	0.79	70	167	0.01	187	0.06	23	2.5
	PdMn/C-BAE	1.031	0.85	79	153	0.29	126	0.24	58	4.0
	PdMn/C-Pol	1.040	0.84	76	152	0.17	114	0.22	44	3.9
15k	**Pd/C-BAE**	1.048	0.82	66	131	0.02	59	0.14	22	3.1
	PdFe/C-BAE	1.020	0.83	81	154	0.31	104	0.15	42	3.9
	PdFe/C-Pol	1.009	0.79	69	146	0.01	55	0.05	16	2.9
	PdMn/C-BAE	1.030	0.84	78	153	0.21	116	0.22	50	3.9
	PdMn/C-Pol	1.036	0.83	77	155	0.14	107	0.20	37	3.8
20k	**Pd/C-BAE**	1.023	0.81	67	134	0.02	51	0.12	18	3.4
	PdFe/C-BAE	1.019	0.83	79	160	0.23	120	0.14	37	4.0
	PdFe/C-Pol	1.000	0.78	70	159	0.01	69	0.04	13	2.6
	PdMn/C-BAE	1.021	0.83	75	160	0.10	107	0.17	37	3.9
	PdMn/C-Pol	1.025	0.82	79	147	0.11	65	0.18	27	3.6

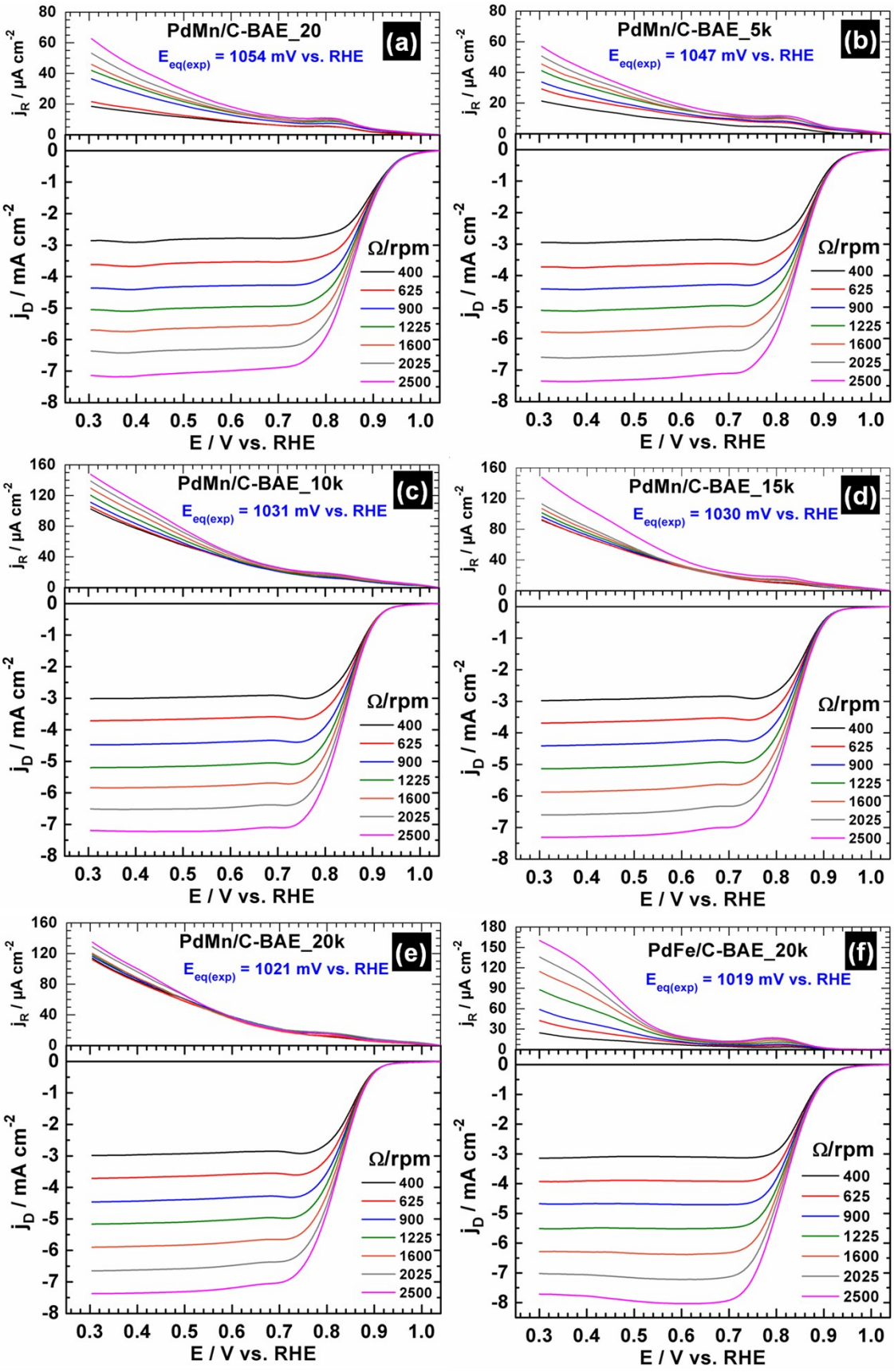

Fig. S2 Typical ORR polarization curves recorded at 5 mV s^{-1} scan rate in O_2-saturated 0.1 mol L^{-1} KOH solution at the ring (top) and disc (bottom) for different speeds of RRDE: **(a)-(e)** PdMn/C-BAE (From 20th to 20,000th APCT) and **(f)** PdFe/C-BAE (20,000th ACPT). For all panels, current densities are obtained with the geometry surface area of the ring (0.110 cm^2) and disc (0.196 cm^2).

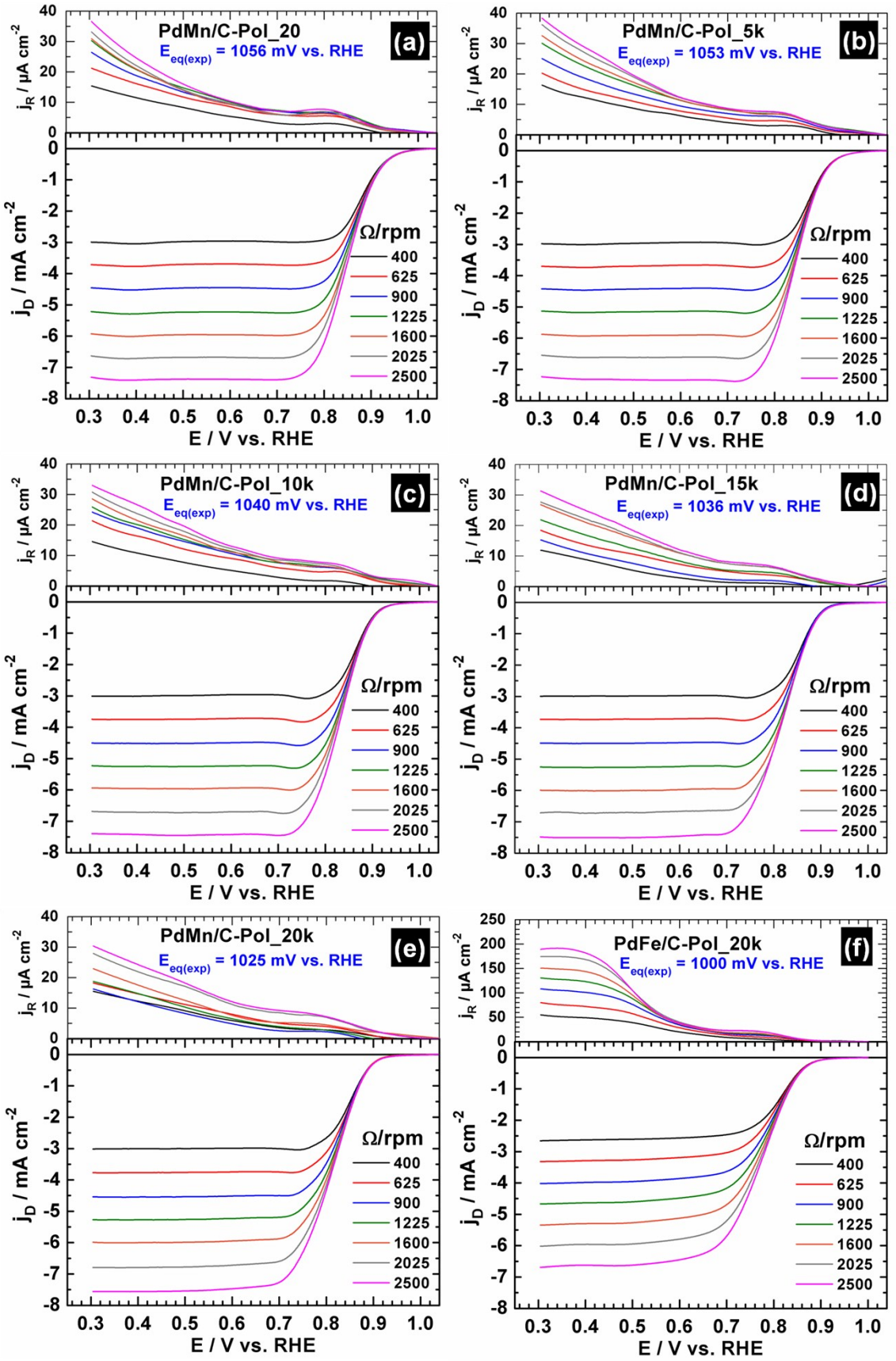

Fig. S3 Typical ORR polarization curves recorded at 5 mV s^{-1} scan rate in O_2-saturated 0.1 mol L^{-1} KOH solution at the ring (top) and disc (bottom) for different speeds of RRDE: **(a)-(e)** PdMn/C-Pol (From 20th to 20,000th APCT) and **(f)** PdFe/C-Pol (20,000th ACPT). For all panels, current densities are obtained with the geometry surface area of the ring (0.110 cm^2) and disc (0.196 cm^2).

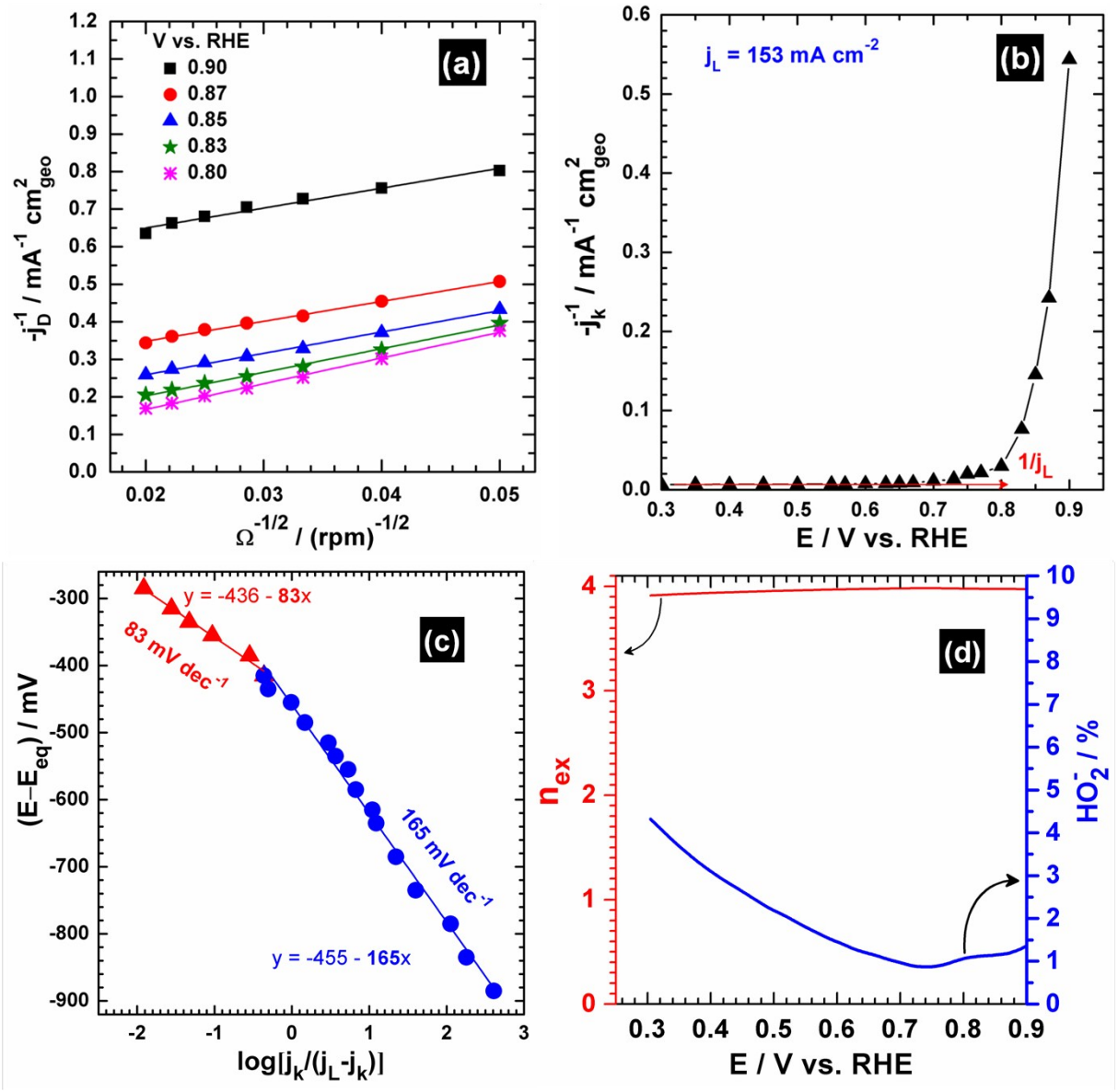

Fig. S4 Typical plots obtained from the ORR polarization curves recorded at 5 mV s^{-1} scan rate: Example for PdMn/C-BAE_20 (after 20th CV) electrode material. **(a)** Koutecky–Levich plots from. **(b)** "j_k^{-1} versus E" plot for the determination of the limiting current density j_L. **(c)** Tafel plots: The limiting current density j_L was determined from the "j_k^{-1} versus potential" plots and a value of E_{eq} = 1.185 V vs. RHE in 0.1 mol L^{-1} KOH was considered. **(d)** HO_2^- (H_2O_2 in acid media) percentage from the incomplete ORR (left *Y*-axis) and the number of electrons exchanged n_{ex} (right *Y*-axis) determined from ORR polarization curves in O_2-saturated 0.1 mol L^{-1} KOH at 5 mV s^{-1} scan rate and RRDE speed of 1600 rpm.

Note: For all panels, the current densities are obtained with the geometry surface area of the ring (0.11 cm^2) and disc (0.196 cm^2).

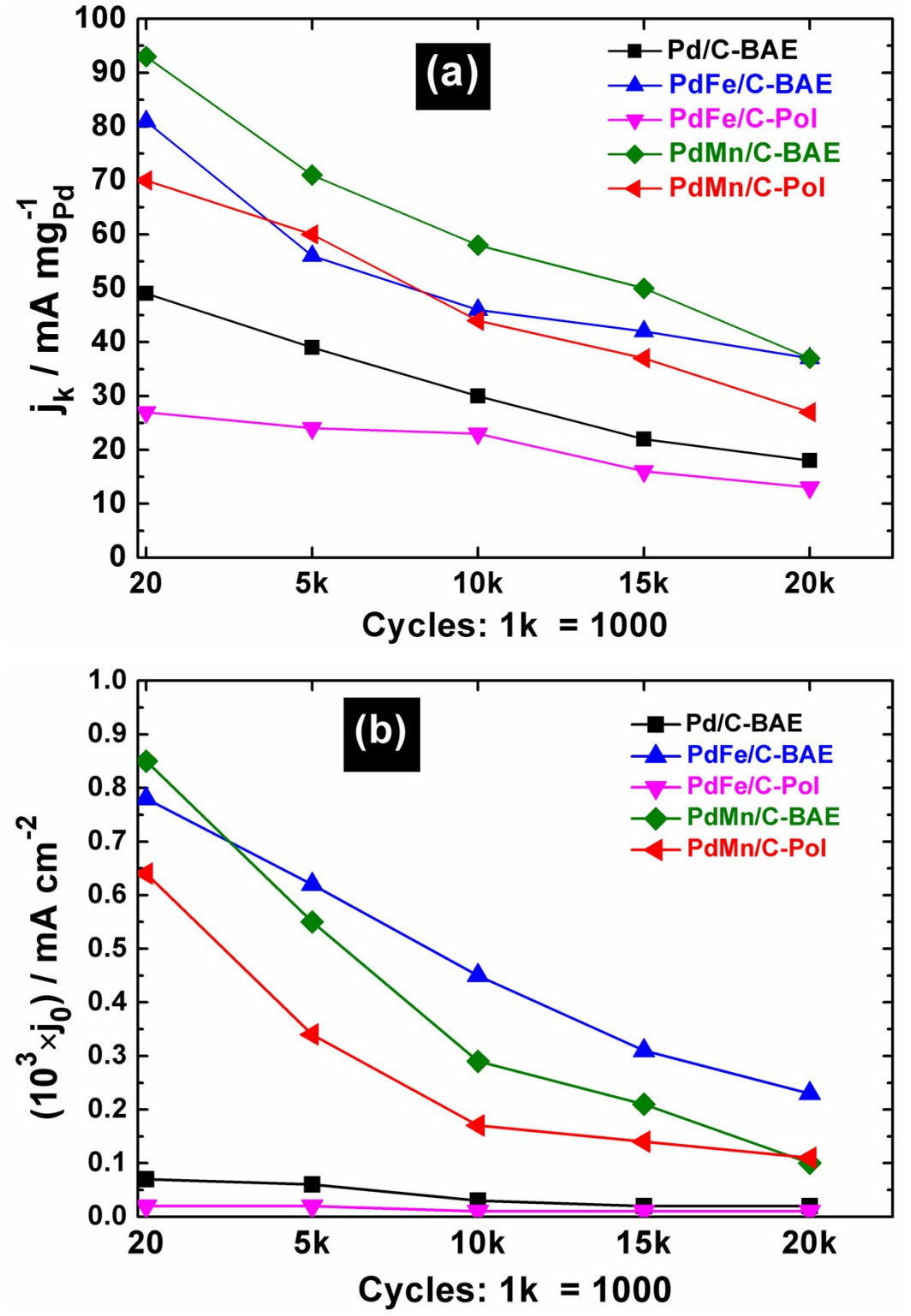

Fig. S5 Kinetic parameters obtained from ORR polarization curves recorded at 5 mV s^{-1} in 0.1 mol L^{-1} KOH during APCT. **(a)** Kinetic current density j_k determined from Koutecky–Levich plots at 0.85 V vs. RHE and referred as "Mass activity" (mA per mg of Pd). **(b)** Exchange current density j_0 (normalized with geometry surface area of the disc: 0.196 cm^2) and determined at low overpotential (high potentials or low currents) where the Tafel slope is 60-85 mV dec^{-1} (Temkin adsorption isotherms of oxygenated species).

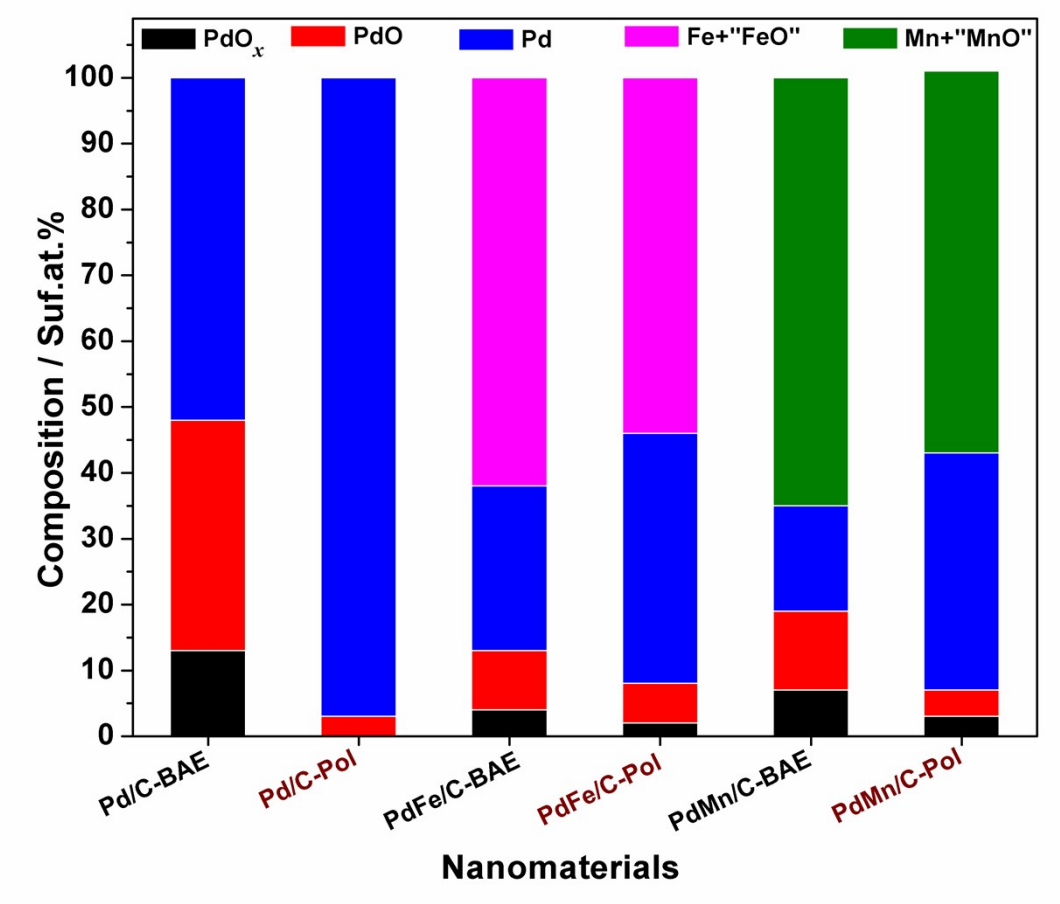

Fig. S6 Surface atomic composition as-determined from XPS.

References

[1] a) S. Trasatti and O. A. Petrii, *J. Electroanal. Chem.* 1992, **327**, 353-376; b) E. Herrero, L. J. Buller and H. D. Abruña, *Chem. Rev.* 2001, **101**, 1897-1930; c) G. Jerkiewicz, *Electrocatalysis* **2010**, **1**, 179-199; d) D. Chen, Q. Tao, L. Liao, S. Liu, Y. Chen and S. Ye, *Electrocatalysis* 2011, **2**, 207-219.

[2] a) N. Tateishi, K. Yahikozawa, K. Nishimura and Y. Takasu, *Electrochim. Acta* 1992, **37**, 2427-2432; b) L. L. Jewell and B. H. Davis, *Appl. Catal. A: Gen.* 2006, **310**, 1-15; c) H. Kobayashi, M. Yamauchi, H. Kitagawa, Y. Kubota, K. Kato and M. Takata, *J. Am. Chem. Soc.* 2008, **130**, 1818-1819; d) D. G. Narehood, S. Kishore, H. Goto, J. H. Adair, J. A. Nelson, H. R. Gutiérrez and P. C. Eklund, *Int. J. Hydrogen Energy* 2009, **34**, 952-960; e) H. Kobayashi, M. Yamauchi, H. Kitagawa, Y. Kubota, K. Kato and M. Takata, *J. Am. Chem. Soc.* 2010, **132**, 5576-5577; f) C.-C. Hu and T.-C. Wen, *Electrochim. Acta* 1995, **40**, 495-503.

[3] M. Grden, M. Lukaszewski, G. Jerkiewicz and A. Czerwinski, *Electrochim. Acta* 2008, **53**, 7583-7598.

[4] Y. Holade, T. W. Napporn, C. Morais, K. Servat and K. B. Kokoh, *ChemElectroChem* **2015**, **2**, 592–599.

[5] X. Ge, A. Sumboja, D. Wuu, T. An, B. Li, F. W. T. Goh, T. S. A. Hor, Y. Zong and Z. Liu, *ACS Catal.* 2015, **5**, 4643-4667.

[6] a) F. J. Vidal-Iglesias, J. Solla-Gullón, A. Rodes, E. Herrero and A. Aldaz, *J. Chem. Educ.* 2012, **89**, 936-939; b) F. Vidal-Iglesias, J. Solla-Gullón, E. Herrero, A. Rodes and A. Aldaz, *Electrocatalysis* 2013, **4**, 1-9.

[7] T. Biegler, R. Woods and *J. Chem. Educ.* 1973, **50**, 604-605.

[8] a) C. Song and J. Zhang, in *PEM Fuel Cell Electrocatalysts and Catalyst Layers* (Ed.: J. Zhang), Springer-Verlag London, London, UK, 2008, pp. 89-134; b) C. Coutanceau, M. J. Croissant, T. Napporn and C. Lamy, *Electrochim. Acta* 2000, **46**, 579-588; c) K. E. Gubbins, R. D. Walker, *J. Electrochem. Soc.* 1965, **112**, 469-471; d) W. Xing, G. Yin and J. Zhang, *Rotating Electrode Methods and Oxygen Reduction Electrocatalysts*, 1 ed., Elsevier Science and Technology, Poland, 2014.

[9] D. Wang, H. L. Xin, R. Hovden, H. Wang, Y. Yu, D. A. Muller, F. J. DiSalvo and H. D. Abruña, *Nat. Mater.* 2013, **12**, 81-87.

[10] a) A. J. Bard and L. R. Faulkner, *Electrochemical Methods: Fundamentals and Applications*, 2nd ed., John Wiley & Sons, Inc., USA, 2001; b) E. Gileadi, *Electrods Kinetics for Chemists, Chemical Engineers, and Materials Scientists*, Wiley-VCH, New York, N Y, USA, 1993.

[11] a) M. K. Debe, *Nature* 2012, **486**, 43-51; b) H. A. Gasteiger, S. S. Kocha, B. Sompalli and F. T. Wagner, *Appl. Catal. B: Env.* 2005, **56**, 9-35.

[12] R. C. M. Jakobs, L. J. J. Janssen and E. Barendrecht, *Electrochim. Acta* 1985, **30**, 1085-1091.

[13] F. T. A. Vork and E. Barendrecht, *Electrochim. Acta* 1990, **35**, 135-139.